1990-12

Investigation of edge effects in thermoacoustic couple measurements

Liu, Wei-Hsin

Monterey, California: Naval Postgraduate School

http://hdl.handle.net/10945/27624

20000831136

NAVAL POSTGRADUATE SCHOOL
Monterey, California

THESIS

Investigation of Edge Effects in Thermoacoustic Couple Measurements

by

Liu, Wei-Hsin

December 1990

Thesis advisor: A. A. Atchley
Co-advisor: T. J. Hofler

Approved for public release; distribution unlimited.

Unclassified

Security Classification of this page

REPORT DOCUMENTATION PAGE

1a Report Security Classification Unclassified	1b Restrictive Markings
2a Security Classification Authority	3 Distribution Availability of Report
2b Declassification/Downgrading Schedule	Approved for public release; distribution is unlimited.
4 Performing Organization Report Number(s)	5 Monitoring Organization Report Number(s)
6a Name of Performing Organization Naval Postgraduate School; 6b Office Symbol *(If Applicable)* PH	7a Name of Monitoring Organization Naval Postgraduate School
6c Address *(city, state, and ZIP code)* Monterey, CA 93943-5000	7b Address *(city, state, and ZIP code)* Monterey, CA 93943-5000
8a Name of Funding/Sponsoring Organization; 8b Office Symbol *(If Applicable)*	9 Procurement Instrument Identification Number
8c Address *(city, state, and ZIP code)*	10 Source of Funding Numbers: Program Element Number; Project No; Task No; Work Unit Accession No

11 Title *(Include Security Classification)* INVESTIGATION OF EDGE EFFECTS IN THERMOACOUSTIC COUPLE MEASUREMENTS

12 Personal Author(s) Liu, Wei-Hsin

13a Type of Report	13b Time Covered	14 Date of Report *(year, month,day)*	15 Page Count
Master's Thesis	From To	December 1990	47

16 Supplementary Notation The views expressed in this thesis are those of the author and do not reflect the official policy or position of the Department of Defense or the U.S. Government.

17 Cosati Codes			18 Subject Terms *(continue on reverse if necessary and identify by block number)*
Field	Group	Subgroup	Acoustics, Thermoacooustics, Thermocoustic Heat Transport

19 Abstract *(continue on reverse if necessary and identify by block number*

Previous measurements of thermoacoustic heat transport across stacks of short plates, called thermoacoustic couples or TACs, revealed serious discrepancies between theory and experiment. The discrepancies are worst at higher drive ratios (the ratio of the peak acoustic pressure amplitude at a pressure antinode to the mean pressure of the gas), where prominent irregularities in the data series appear. In the previous work, the measurements were made with thermopiles having junctions that were located along the leading and trailing edges of the TAC plates. Because of its proximity to the edge, the thermopile may have been sensitive to effects which, though perhaps causing *local* deviations in the temperature profile, do not affect the temperature profile in interior regions of the plate. To investigate whether edge effects are the cause of any of these discrepancies, we have constructed a TAC with two thermopile, whose junctions do not lie along the edge, and repeated some of the previous measurements. Measurements were also made with a stack of long plates to probe how far the irregularities extend in to the interior of the plate. It was found that the irregularities are not isolated to the edge of the TAC. The temperature profile of interior portions of the plates mimic that measured along the edge.

20 Distribution/Availability of Abstract [X] unclassified/unlimited [ ] same as report [ ] DTIC users	21 Abstract Security Classification Unclassified
22a Name of Responsible Individual Anthony A. Atchley	22b Telephone *(Include Area code)* (408) 646-2848; 22c Office Symbol PH/Ay

DD FORM 1473, 84 MAR | 83 APR edition may be used until exhausted | security classification of this page

All other editions are obsolete | Unclassified

Approved for public release; distribution is unlimited.

Investigation of Edge Effects in Thermoacoustic Couple Measurements

by

Liu, Wei-Hsin
Cdr, Republic of China Navy
B.S., Chinese Naval Academy, 1978

Submitted in partial fulfillment of the
requirements for the degree of

MASTER OF SCIENCE IN ENGINEERING ACOUSTICS

from the

NAVAL POSTGRADUATE SCHOOL
December 1990

Author: [redacted]
Liu, Wei-Hsin

Approved by: [redacted]
Anthony A. Atchley, Thesis Advisor

[redacted]
Thomas J. Hofler, Thesis Co-advisor

[redacted]
Anthony A. Atchley
Chairman, Engineering Acoustics Academic Committee

ABSTRACT

Previous measurements of thermoacoustic heat transport across stacks of short plates, called thermoacoustic couples or TACs, revealed serious discrepancies between theory and experiment. The discrepancies are worst at higher drive ratios (the ratio of the peak acoustic pressure amplitude at a pressure antinode to the mean pressure of the gas), where prominent irregularities in the data series appear. In the previous work, the measurements were made with thermopiles having junctions that were located along the leading and trailing edges of the TAC plates. Because of its proximity to the edge, the thermopile may have been sensitive to effects which, though perhaps causing *local* deviations in the temperature profile, do not affect the temperature profile in interior regions of the plate. To investigate whether edge effects are the cause of any of these discrepancies, we have constructed a TAC with two thermopile, whose junctions do not lie along the edge, and repeated some of the previous measurements. Measurements were also made with a stack of long plates to probe how far the irregularities extend in to the interior of the plate. It was found that the irregularities are not isolated to the edge of the TAC. The temperature profile of interior portions of the plates mimic that measured along the edge.

TABLE OF CONTENTS

LIST OF TABLES

LIST OF FIGURES

LIST OF SYMBOLS

c	sound speed
c_p	isobaric heat capacity per unit mass of the gas
c_s	isobaric heat capacity per unit mass of the solid
d_g	plate separation
d_{fg}	thickness of fiberglass plate
d_p	plate thickness
d_{ss}	thickness of stainless steel plate
f	frequency
k	propagation constant
P_o	peak acoustic pressure amplitude
T_m	mean gas temperature
u_o	peak acoustic velocity
x	distance from rigid end of tube to center of plate
γ	ratio of specific heats
δ_k	thermal penetration depth in the gas
δ_s	thermal penetration depth in the plate
δ_v	viscous penetration depth in the gas
ΔT	temperature difference
Δx	TAC length
k_g	thermal conductivity of gas
k_{fg}	thermal conductivity of fiberglass

LIST OF SYMBOLS (CONTINUED)

k_p	thermal conductivity of the plate
k_{ss}	thermal conductivity of the stainless steel
λ	acoustic wavelength
μ	dynamic viscosity of the gas
ν	kinematic viscosity of the gas
ρ_m	mean gas density
σ	Prandtl number
ω	angular frequency

ACKNOWLEDGEMENTS

First and foremost, I would like to express my sincere appreciation to my advisors, Dr. Anthony Atchley and Dr. Thomas Hofler for their great assistance, words of wisdom, and infinite patience. Without their capable hands and clever escort, I would still be in the basic phase of the experiment.

Next, I thank Mr. Steve Blankschein and George Jaksha of the physics department machine shop. His unparalleled ability and insight into my poorly worded construction requests in precisely made apparatus which enabled me to conduct my experiment.

Finally, I thank my wife, li-tsun. During the last two and half years, I didn't spent any time to help my family, however, was her understanding, patient and also my farsighted view eleven years ago.

I. INTRODUCTION AND BACKGROUND

A thermoacoustic heat pump converts acoustic energy into stored thermal energy, in the form, for example, of a temperature difference across a plate situated in an acoustic standing wave. The operation of a heat pump can be explained in rather simple terms. Figure 1 is a simplified illustration of the basic thermoacoustic effect. It shows a short, thin, poorly thermally conducting plate situated near the rigid end of a resonator. Initially the plate is at a uniform temperature T. We isolate our attention to the gas within a thermal penetration depth of the plate as an acoustic standing wave is established in the tube. Viscous effects are ignored. During the compression phase of the acoustic cycle, the gas parcel is compressed and displaced toward the pressure antinode. As a result of the compression the temperature increases from T to T^{++}. Because the gas is now hotter than the portion of the plate below it, an amount of heat dQ flows from the gas parcel to the plate. The temperature of the gas parcel drops from T^{++} to T^{+}. During the expansion phase of the acoustic cycle, the gas parcel undergoes an expansion and returns to its initial position. As a result of the expansion, the parcel's temperature decreases from T^{+} to T^{-}. Now the parcel is cooler than the portion of plate immediately below it. A second irreversible heat flow occurs, this time from the plate to the parcel. This heat flow returns the parcel to its initial temperature. The net result of this cycle is the transport of heat toward the pressure antinode, resulting in a temperature difference across the TAC.

Wheatly, et al [Ref. 1]. derived an expression for the steady state temperature difference developed across a TAC in an acoustic standing wave.

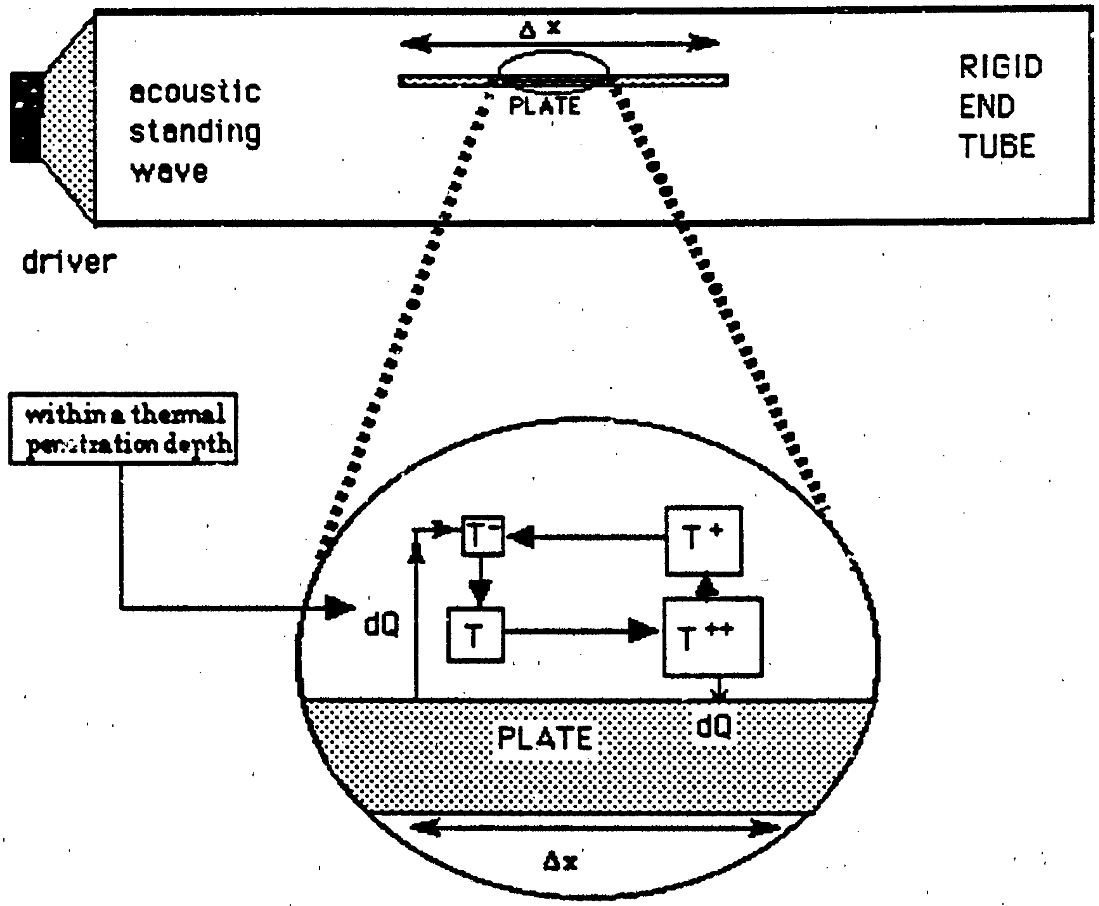

Figure 1 - A simplified illustration of the thermoacoustic effect.

$$\Delta T = \left(\frac{1}{4}\frac{P_o^2\delta_k(1+\sqrt{\sigma})\sin 2kx}{\rho_m c\left[(k_p d_p + k_g d_g)/\Delta x\right](1+\sigma)}\right)$$
$$\times\left(1+\frac{1}{4}\frac{P_o^2\delta_k(1-\sigma\sqrt{\sigma})(1-\cos 2kx)}{\left[(k_p d_p + k_g d_g)/\Delta x\right]\rho_m \Delta x T_m \omega(\gamma-1)(1-\sigma^2)}\right)^{-1}. \qquad (1)$$

The thermal penetration depth is defined as

$$\delta_k = \sqrt{2\kappa_g / \rho_m c_p \omega}\ . \tag{2}$$

The viscous penetration depth is defined as

$$\delta_v = \sqrt{2\mu / \rho_m \omega}\ . \tag{3}$$

The Prandtl number is defined as

$$\sigma = c_p \mu / k\ . \tag{4}$$

A useful equation relating the Prandtl number and the penetration depth is

$$\sigma = \left(\delta_v / \delta_k \right)^2 . \tag{5}$$

The term $k_p d_p$ in Eq. (1) will be a function of the geometric and thermal properties of the plate used in the TAC construction. For the G- 10 fiberglass and stainless steel laminated plates used in a portion of the measurements

$$k_p d_p = (2k_{fg} d_{fg} + k_{ss} d_{ss}) \tag{6}$$

For stainless st :el plates

$$k_p d_p = k_{ss} d_{ss}. \tag{7}$$

The first measurement of the thermoacoustic effect was performed by Wheatly, et. al. [Ref. 1]. In particular, they measured the temperature difference developed across a short stack of plates, called a ThermoAccustic Couple (or TAC) as a function of its position in an acoustic standing wave. At low drive ratios (the ratio of the peak acoustic pressure to the mean gas pressure), they found that the temperature difference across the TAC is a nearly sinusoidal function of its position in the standing wave. Zeros in the temperature difference occur at both pressure and velocity nodes. Also, the hot end of the TAC is always closer to the nearest pressure antinode. Although they developed a theoretical expression for the temperature difference, Wheatly, et. al. attempted little quantitative comparison of their results with theory. In 1987, a quantitative investigation of thermoacoustic heat transport was undertaken in the physics department at the Naval Postgraduate School [Ref. 2]. They measured the temperature difference developed across various TACs as a function of their position in the acoustic field, the drive ratio (extended to high drive ratio), the plate configuration, the thermal properties of the plate, and the thermophysical properties of the gas.

Specific examples of previous NPS research are presented in Figs. 2 and 3. They are graphs of the predicted (Fig. 2) and measured (Fig. 3) temperature difference developed across a TAC for various drive ratios as a function of kx. Of particular interest are the irregularities in the measured data series apparent at higher drive ratios. The minimum value of the drive ratio required for these irregularities to appear is approximately 1%. The dashed curve in Fig. 3 represents the highest drive ratio for which irregularities are not present. It corresponds to a drive ratio of 1.03%.

In order to quantify the comparison of the data shown in Figs. 2 and 3, three ratios were examined. The first ratio is that of the experimental slope of the ΔT curve in the vicinity of the velocity antinode to the theoretical slope in the vicinity of the velocity antinode. The second ratio is the ratio of the experimental to theoretical slope of the ΔT curve in the vicinity of the pressure antinode. The final ratio is that of the maximum experimental temperature difference to the maximum theoretical temperature difference. As seen in Figs. 2 and 3, ΔT reaches a maximum on both sides of the pressure antinode, so two values of the maximum ΔT ratio can be computed. The ratios just described are plotted as functions of the drive ratio (in %) in Fig. 4 for the data presented in Figs. 2 and 3. The mean gas pressure is approximately 114 kPa.

All ratios have approximately the same value for drive ratios less than approximately 0.5%. The ratios then start to decrease in a more-or-less linear fashion for drive ratios up to approximately 1.1%. At this point the quasilinear decrease stops. The reader should recall that the data for the drive ratio of 1.03% correspond to the dashed curve in Fig. 3 which demarcates the regions of regular and irregular behavior of the ΔT data series. As the drive ratio increases beyond approximately 1.1%, the pressure antinode slope ratio increases slightly and then levels off at a drive ratio of approximately 1.5%. In the drive ratio region above 1.0%, the maximum ΔT ratios more-or-less level off, whereas the velocity antinode slope ratio tends to decrease, though at a slower rate than in the 0.5 to 1.1% drive ratio region.

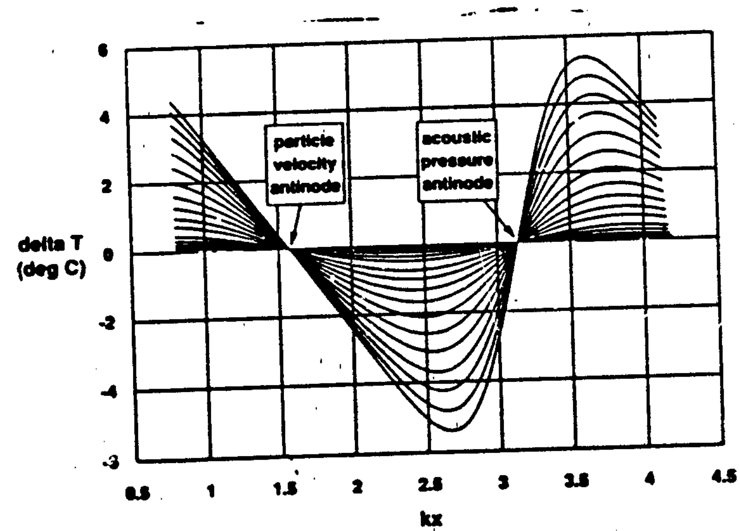

Figure 2- Graph showing the theoretical temperature difference as a function of kx for drive ratio from 0.17% to 1.99% (Fig 10 from Ref. 2).

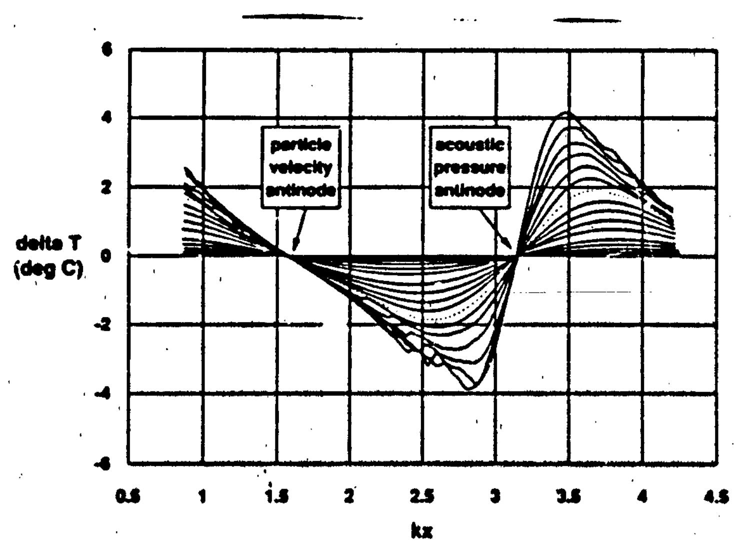

Figure 3 - Graph showing the measured temperature difference as a function of kx for drive ratio from 0.17% to 1.99% (Fig 11 from Ref. 2)

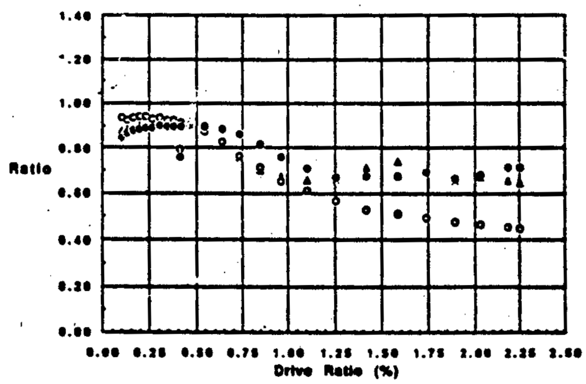

Figure 4 - Graph showing the dependence of of the three ratios on drive ratio (in %) (Fig 12 from Ref. 2)

Atchley et al [Ref. 2] cited two plausible explanations for the behavior described above. One argument is that the acoustic particle displacement is a sizeable fraction of the TAC length, at the highest drive ratios. A drive ratio of 2% results in a peak particle displacement of approximately 3 mm. At these extreme drive ratios, the gas parcels having equilibrium positions within 1.5 mm or so of the edge of the plate do not fully participate in the heat transport process. Another effect that could account for the observed discrepancy between measurement and theory is boundary layer turbulence. However, based on calculation of Reynolds numbers, it seems unlikely that true boundary layer turbulence existed in their system. However, Reynolds numbers based on larger characteristic lengths such as the size of the TAC itself or the probe tube standoff, are much larger and may in fact cause turbulent flow.

How these situations might affect the value of the temperature difference measured between the edges of the TAC is not obvious. However, the temperature difference was measured with thermopiles having junctions that were located along the leading and trailing edge of the TAC plates. Because of its proximity to the edge, the thermopile may be sensitive to effects which, though perhaps causing *local* deviations in the temperature profile, do not affect the temperature profile in interior regions of the plate. In other words, although considerable deviations are observed between theory and measurements made at the plate edges, the interior (and majority) of the plate may behave in accordance with predictions. Therefore, useful information might be gained by locating the junctions of the thermopile well away from the edges of the TAC, in order to avoid edge effects. The results of such measurements are reported in this thesis.

II. EXPERIMENT APPARATUS AND PROCEDURE

The discussion of the apparatus will be divided in to the following sections: the TACs; the TAC probe; the resonator tube and the acoustic driver housing; the TAC positioning system; and the electronic equipment. A complete description of the experimental apparatus is given in Ref 2.

A. THERMOACOUSTIC COUPLES (TAC)

Three TACs were used in these measurements. They will be refereed to as TAC#1, TAC#2 and TAC#3, respectively. The general construction of the TACs is illustrated in Figure 5, 6 and 7. The design of the first two TACs and the materials used in their construction were dictated by the desire to make the TACs similar to those used by Atchley et al. [Ref. 2] TAC#3 is much longer than the others. The specifications of the TACs are given in Tables 1, 2 and 3. From Figure 5, each TAC is a five-plate stack, consisting of a central plate surrounded by four guard plates. The purpose of the guard plates are both to provide a well-defined path for longitudinal thermal conduction through the gas, described by the $k_g d_g$ term in Eq. (1), and to reduce the effect of transverse thermal conduction from plate to plate.

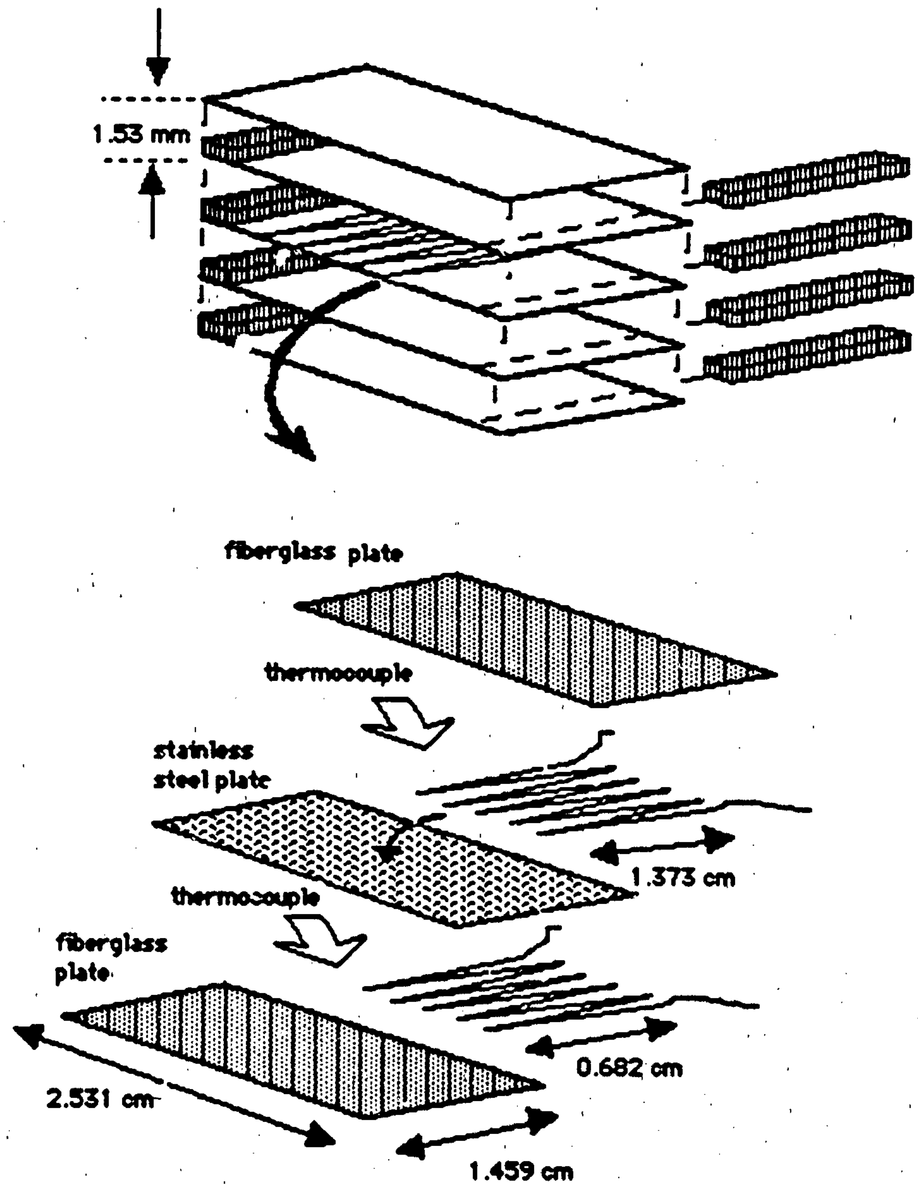

Figure 5 - TAC#1 configuration

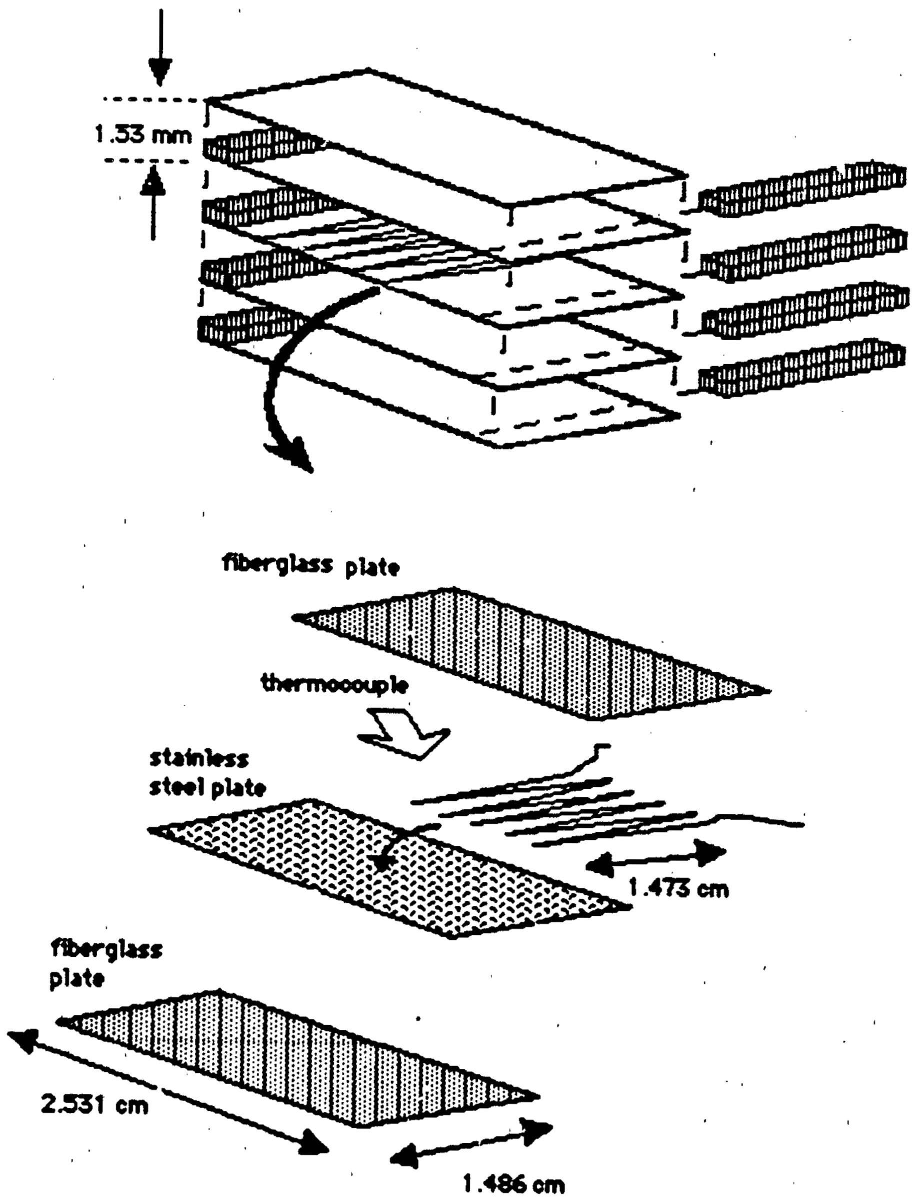

Figure 6 - TAC#2 configuration

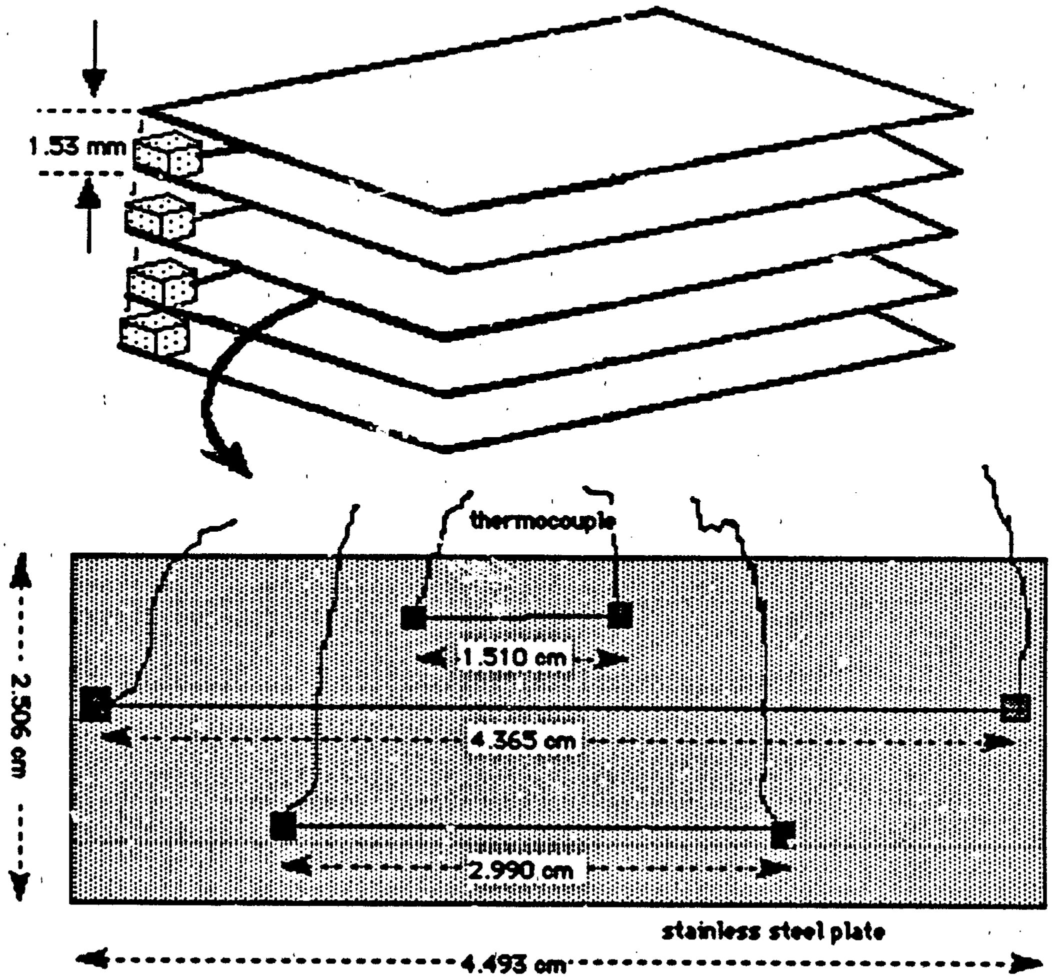

Figure 7 - TAC#3 configuration

TABLE 1: SPECIFICATIONS OF TAC#1

Upper and lower layer	• G-10 fiberglass • Size: 1.495 cm long, 2.531 cm wide, 0.131mm thick • Thermal conductivity: 0.48 W/mK
Middle layer	• AISI-302 stainless steel • Size: 1.495 cm long, 2.531 cm wide, 0.105 mm thick • Thermal conductivity: 11.8 W/mK
Thermopile junction pairs number: 5 Thermocouple wire diameter: 0.0254 mm Number of plate: 5 Spacing in between any two adjacent plate: 1.53 mm Length of thermocouple: outer thermopile: 1.373 cm inner thermopile: 0.682 cm	

TABLE 2: SPECIFICATIONS OF TAC#2

Upper and lower layer	• G-10 fiberglass • Size: 1.486 cm long, 2.531 cm wide 0.131 mm thick • Thermal conductivity: 0.48 W/mK
Middle layer	• AISI-302 stainless steel • Size: 1.478 cm long, 2.531 cm wide, 0.105 mm thick • Thermal conductivity: 11.8 W/mK
Thermopile junction pairs number: 5 Thermocouple wire diameter: 0.0254 mm Number of plate: 5 Spacing in between any two adjacent plate: 1.53 mm Length of thermocouple: 1.473 cm	

TABLE 3: SPECIFICATIONS OF TAC#3

Stainless steel plate	• AISI-302 stainless steel •Size: 4.493 cm long, 2.506 cm wide, 0.105 mm thick •Thermal conductivity: 11.8 W/mK
Thermopile junction pairs number: 1 Thermocouple wire diameter: 0.0254 mm Number of plate: 5 Spacing in between any two adjacent plate: 1.53 mm	
Length of thermocouple: • outer thermopile: 4.365 cm • middle thermopile: 2.99 cm • inner thermopile: 1.51 cm	

The plates comprising TAC#1 and #2 are a lamination of three plates (one 302 stainless steel and two G-10 fiberglass) epoxied together. The plates are separated by approximately 1.53 mm. The central plate of each stack is instrumented with either one or two thermopiles, consisting of five thermocouple junctions connected in series. The thermopiles are epoxied between these three plates. The fiberglass lamination ensures that the plate surface is smooth. The purpose of the thermopile is to provide measured sensitivity over a single thermocouple for measuring the temperature difference developed across the TAC. The temperature difference is determined by measuring the voltage output of the thermopile and dividing by the the number of junction pairs and sensitivity (in V/°C) of the particular type of thermocouple. Type E chromel-constantan thermocouples are used in these measurements.

B. TAC PROBE

The probe is illustrated in Figure 8. The TAC is mounted on the end of a hollow 1/8-in.-o.d. stainless steel tube, called the TAC probe. The wires pass through the hollow tube and exit into the tail section of the probe. A pressure-tight feed through connector is connected to the probe tube, which allows for external electrical connections without loss of pressure in the resonator tube and driver housing. The TAC probe passes through a pressure tight O-ring connector located in the closed end of the resonator tube.

C. RESONATOR TUBE AND ACOUSTIC DRIVER HOUSING

The resonator tube and acoustic driver housing are sketched on Figure 9. The standing wave is generated with a JBL model 2445J compression driver located within a pressure housing. The driving housing is bolted via a brass flange to the end of a 1.22-m-long 3.8-cm-i.d. copper tube, called resonator tube. The other end is also flanged. A brass plate is bolted to this flange and forms the closed end of the resonator. This brass plate contains the connector through which the TAC probe passes. It also houses an Endevco model 8510B-5 high-intensity pressure transducer, which is used to monitor the acoustic pressure at the closed end. The entire length of the resonator is surrounded by a 7.6-cm-i.d. brass tube. Water is circulated, with a Neslab model RTE-110 circulation temperature control bath, through the region between the two tubes in order to maintain a uniform temperature along the resonator tube. The water is also circulated around the driver housing through flexible plastic tubing. A layer of cloth insulation is wrapped around the outside of the tubing. A tee connection for evacuating and filling the resonator/driver

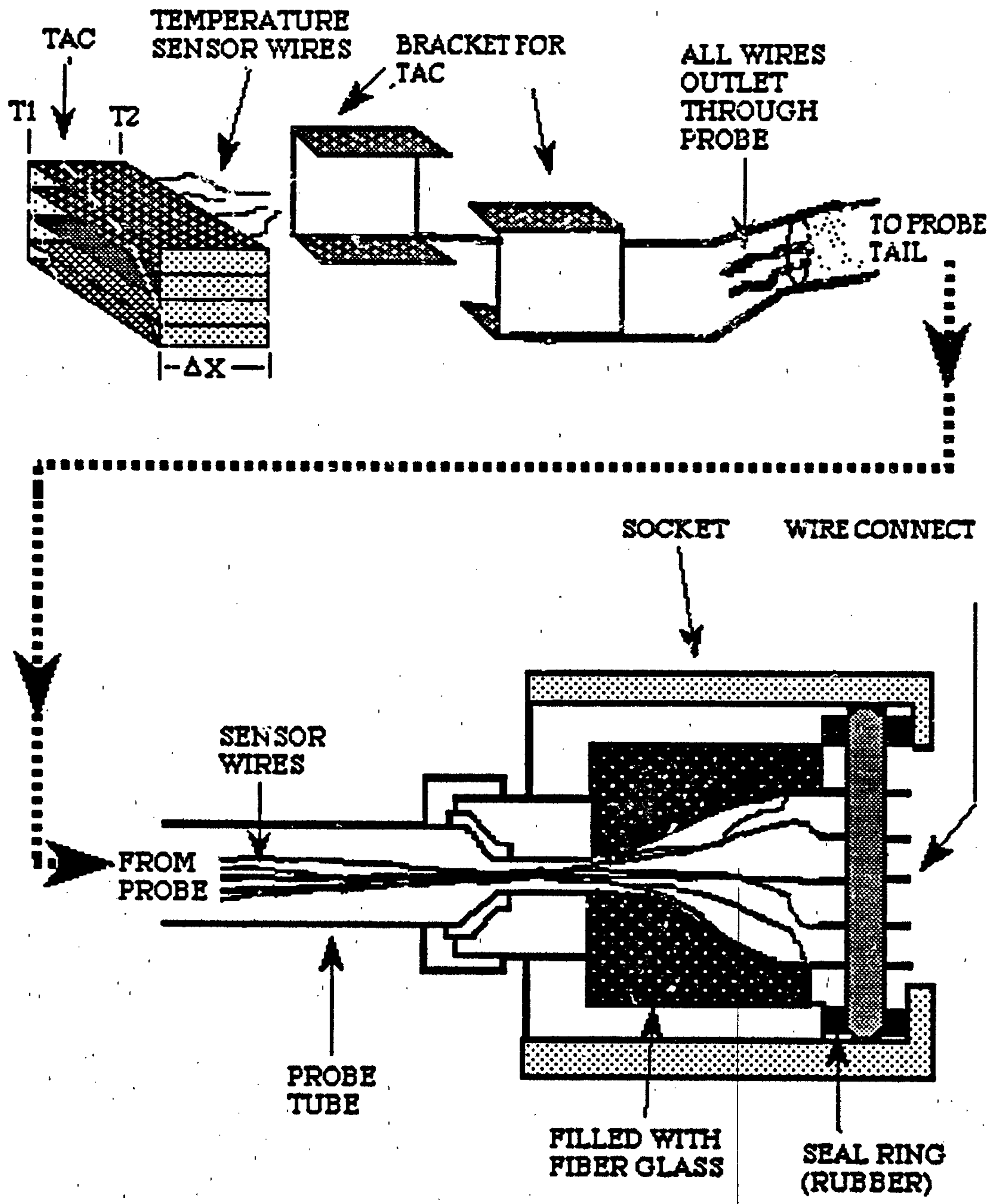

Figure 8 - TAC mounting bracket and TAC probe

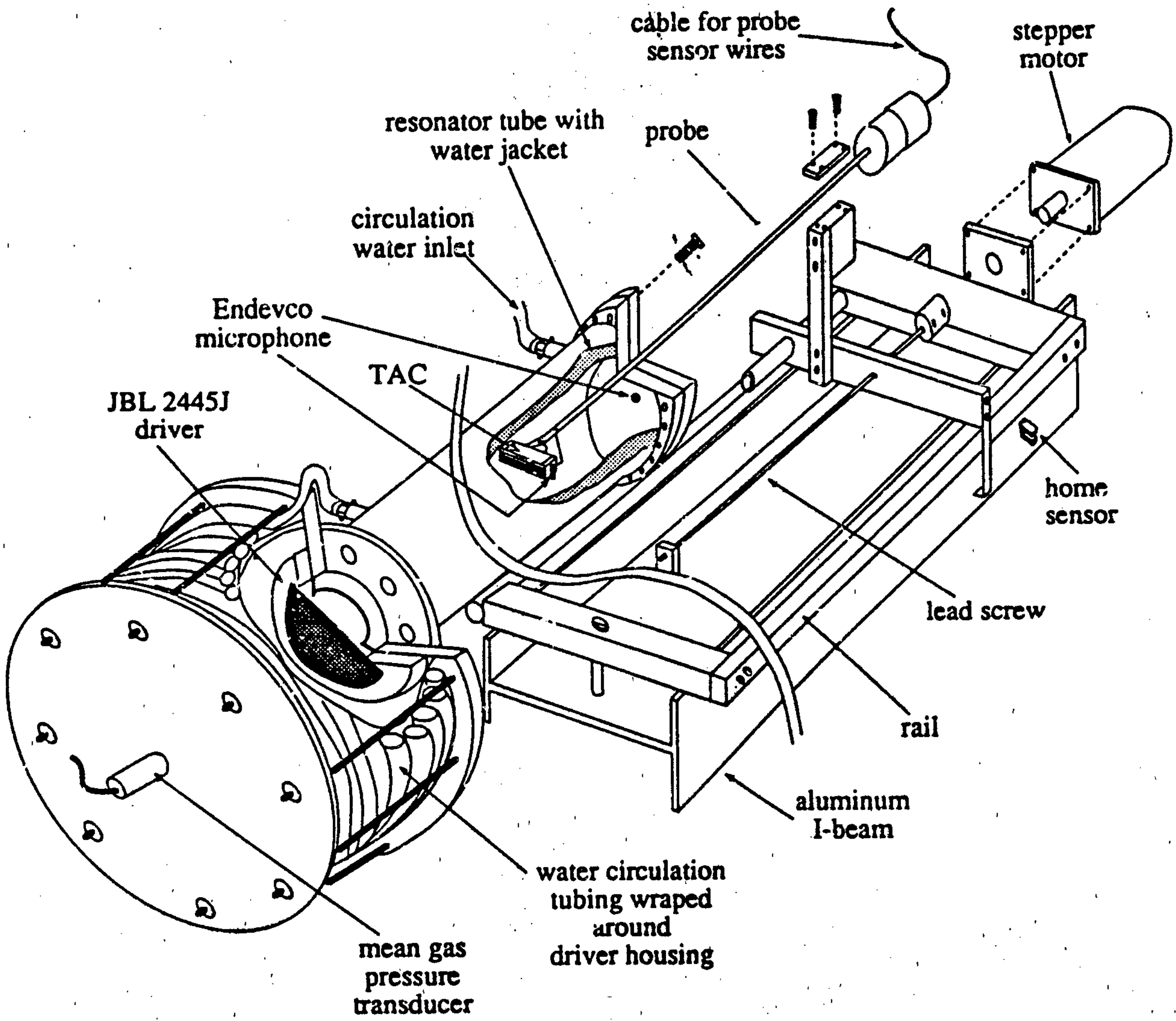

Figure 9 - Illustration of the resonator and the driver housing

housing is provided via an 1/8-in.-diam copper tube. One end of the tee is connected to a longer fill tube leading to the gas /vacuum system. Another end of the tee is soldered to the resonator near the driver housing end of the resonator. The final end of the tee goes to the driver housing. Having the resonator and driver housing connected through the tubing prevents a substantial pressure difference from being established across the driver diaphragm during the evacuation/pressurization sequence. The driver house is fitted with a pressure relief valve that prevents pressurization of the system beyond safe limits.

An example of the waveform measured at the rigid end of the resonator, along with its spectrum, are shown in Fig. 10 and 11. The drive ratio is 2.32%. The fundamental resonance frequency is 700 Hz. It can be seen that the second harmonic is approximately 27 db below the fundamental.

D. TAC POSITIONING SYSTEM

The TAC is positioned within the resonator with a Compumotor model M83-135 computer-controlled stepper motor and indexer as depicted in Figure 12. The positioning system allows a maximum travel of approximately 76 cm. It is desired to be able to cover one complete temperature difference cycle with the measurements. By operating the resonator in the third mode this 76 cm travel is sufficient to cover one thermoacoustic cycle.

E. ELECTRONIC EQUIPMENT

The diagram of the electronic instrument is shown in Figure 10. The experiment was controlled with a Standard 286 IBM AT compatible computer. The HP 3314 function generator, HP 3457 multimeter, and the stepper motor

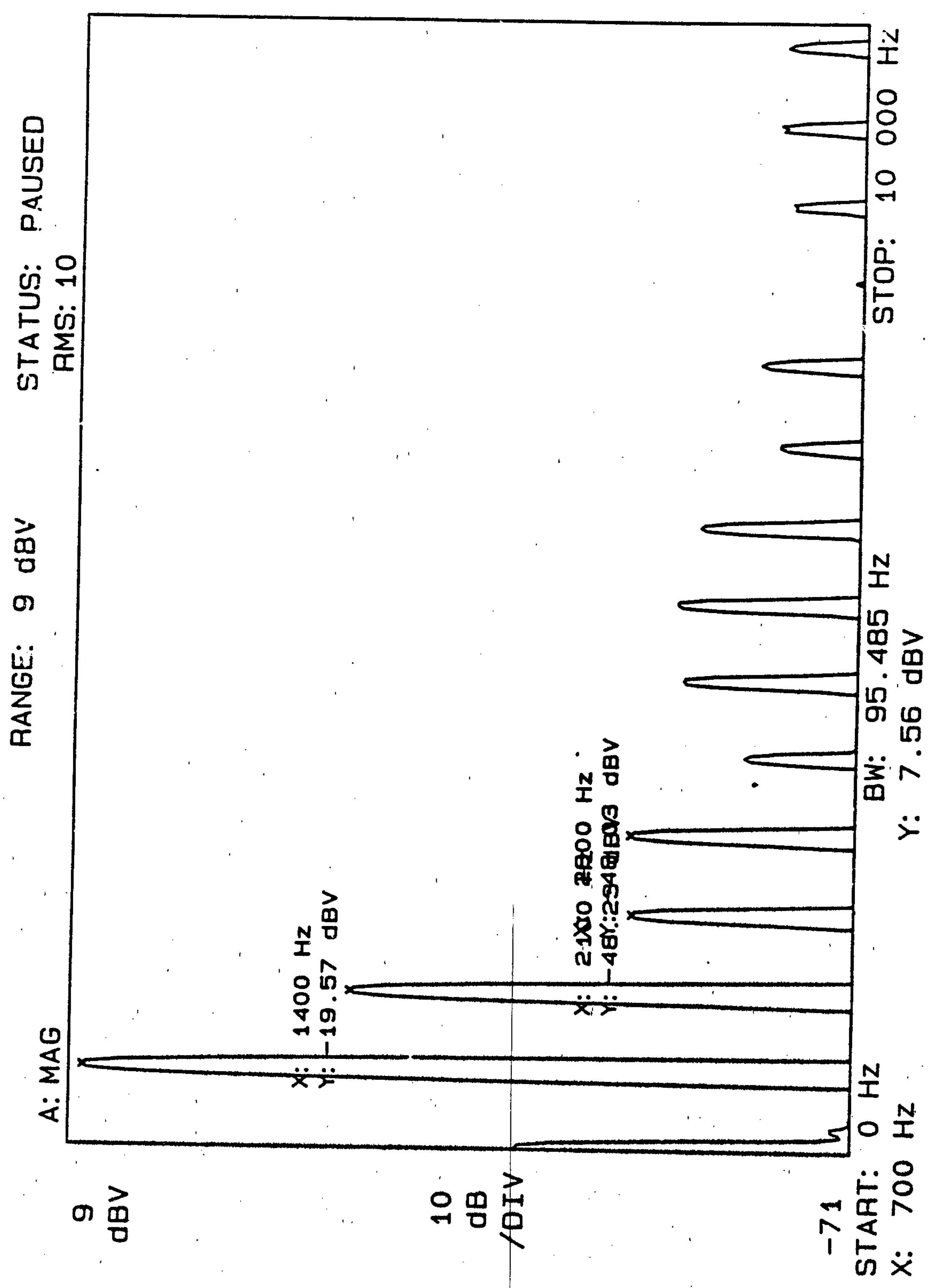

Figure 10 - The pressure signal component in the tube at drive ratio 2.32%

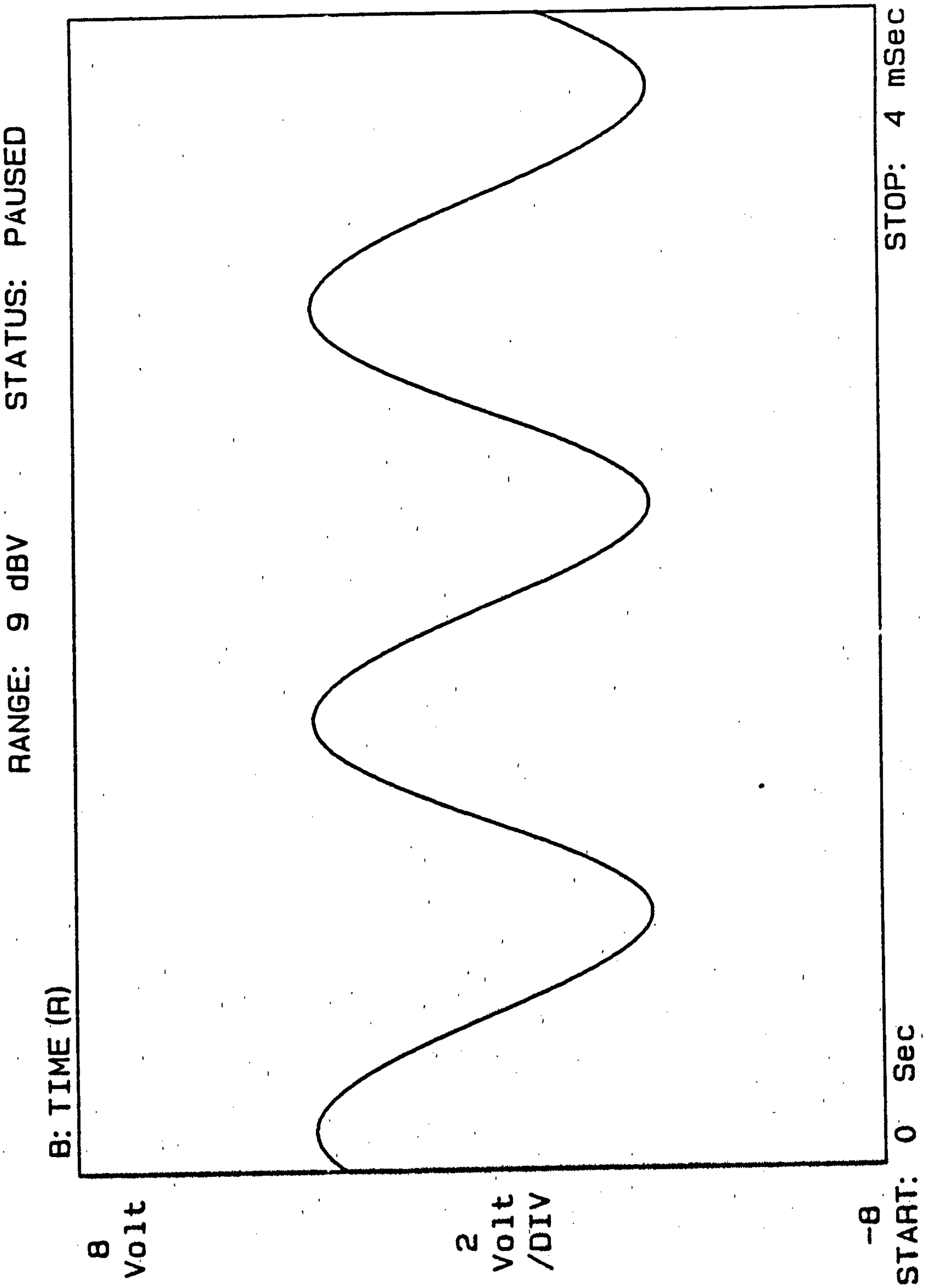

Figure 11 - The pressure standing wave in the tube at drive ratio 2.32%

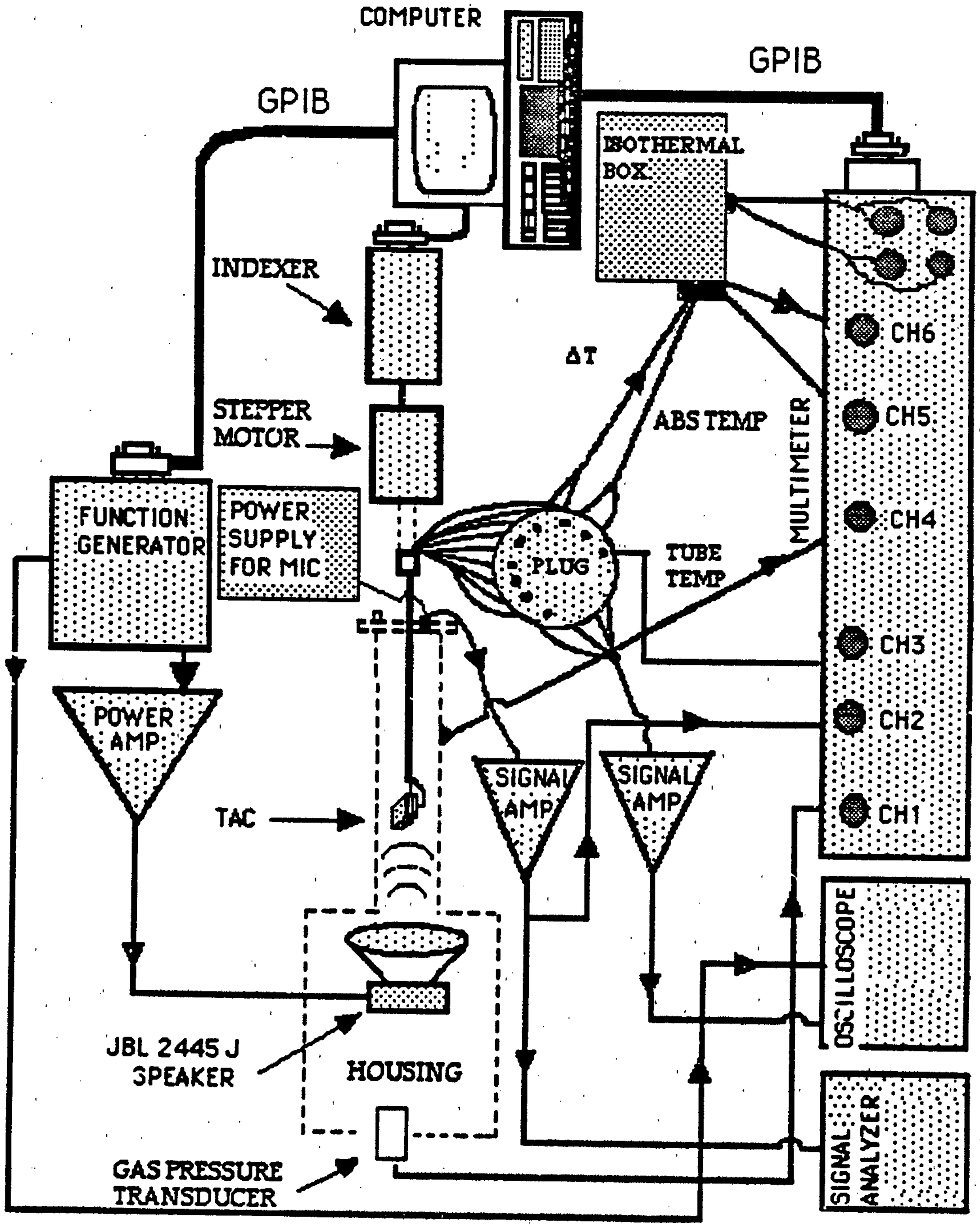

Figure 12 - Schematic diagram of the data acquisition system

indexer were controlled with a GPIB interface. The control program was written in Microsoft QuickBASIC. The program set the amplitude and frequency of the function generator, instructed the indexer when to move the TAC, and recorded all of the data from the HP 3457 multimeter. An TEKTRONIX 2445A oscilloscope was used to monitor the acoustic signal via a Endevco transducer mounted on the right end of the tube. An HP 3561 dynamic signal analyzer was used to determine the proper operating frequency. An HP plotter and printer were also connected to the GPIB interface to print the data. Two different amplifiers were used in this experiment. A TEKTRONIX 2445A differential amplifier was used to amplify for the output from the wall mounted transducer. An OSC audio MODEL 1700 amplifier was used to drive the JBL compression speaker.

F. EXPERIMENTAL PROCEDURE

Prior to data acquisition, the following procedures are conducted. The water circulator is started and then allowed to come to the set point temperature, which is monitored at the middle of the resonator tube. The gas used in this experiment is helium. To minimize contamination of the resonator with air, the resonator and driver housing are evacuated to less than 1% of atmospheric pressure and then filled with helium. This procedure is repeated twice and then filled with helium to two atmospheres pressure. Next, the function generator was adjusted to a frequency near resonance. Then the power amplifier input is connected to the function generator output and the amplifier gain set to the proper level to drive the JBL compression speaker.

Data acquisition is accomplished as follow. First, the computer records the mean gas pressure, the voltage difference across the TAC, and the temperature reference. The measured voltage is converted to a temperature difference using a low-order polynomial, fit over a limited temperature range to data obtained from an NBS Thermocouple Table. Second, is the TAC position relative to the rigid end. The TAC is then moved in 0.7-cm increments. After the TAC position is incremented, a 45-s wait period is initiated before the next data acquisition. The duration of the wait time was required for the temperature difference across the TAC to come to steady state.

III. RESULTS AND DISCUSSION

In this chapter the result of two phases of experiment will be present and discussed. The first phase is devoted to investigating "edge effects". The next phase involved measuring the temperature difference developed across a long stack of plates. The purpose was to investigate the extent to which irregularities in the temperature difference extend into the plate interior.

A. EDGE EFFECT

We constructed a TAC (TAC#1) with two thermopiles, whose junctions do not lie along the edge, and repeated some of the measurements made previously by Atchley et al [Ref. 2]. The results are shown in Figs. 13 and 14, TAC #1 is 1.495 cm long. The two thermopiles are 1.373 cm and 0.682 cm long and centered on the TAC. Therefore, the thermocouple junction lie approximately 0.061 cm and 0.407 cm from the edge, respectively. Figure 13 shows the data from the longer thermopile, Fig. 14 from the shorter. The TAC is in helium at a mean gas pressure and temperature of 200 ± 1 kPa and 295.9 ± 0.1° K. The frequency range for the data is 662.8±4.5 Hz. The drive ratio range is 0.20% - 2.70%. The dashed curve in both figures corresponds to a drive ratio 0.97%. (Recall that the dashed curve in Fig. 3 corresponds to a drive ratio of 1.03%.) Comparing these results with those shown in Fig. 3, they are strikingly similar. (No direct comparison is possible since the experimental condition are different.) Moreover, the transition to an irregular behavior starts at a 1% drive ratio, as it did with the edge-to-edge design. These data show that the temperature profile of the interior of the

T'.C behaves the same as that measured at the edge. Therefore, the irregularities previously observed are not an artifact of placing the thermopile along the edge. The irregularities may still be the result of the edge (e.g., turbulence generated at the edge), but they are not isolated to the edge. They extend at least half way to the center of the TAC.

One point should be clarified. In Figure 13, all of the curves should pass through zero both at velocity antinode and pressure antinode. In the graph at kx about 3.1 (the pressure antinode) some ΔT curves did not pass the zero. This behavior is the result of a temporary malfunction in the power supply of the stepper motor during the data acquisition. The indexer did not proceed properly.

As with Atchley et al, we examined four ratios derived from the measured and theoretical value of ΔT, the results are presented in Figure 17 and 18. They are

Ratio 1: the experimental slope of the ΔT curve in the vicinity of the velocity antinode to the theoretical slope in the vicinity of the velocity antinode. (The + marker on graph).

Ratio 2: the maximum measured negative temperature difference to the maximum theoretical negative temperature difference. (The open squares marker).

Ratio 3: the experimental slope of the ΔT curve in the vicinity of the pressure antinode to the theoretical slope in the vicinity of the pressure antinode. (The o marker).

Ratio 4: the maximum measured positive temperature difference to the maximum experimental positive temperature difference. (The * marker).

They overall dependence on drive ratio is the same for the two thermopiles, although the ratio in Fig. 18 about 0.1 lower than those in Fig. 17. Also, three regions of behavior are evident as in Fig. 4. However the drive ratios at the transitions between these regions are higher than those in Fig. 4. Furthermore the transition between the second and third regions is not as distinct.

B. MEASUREMENTS WITH A LONG STACK

The results of the previous section indicate that the irregularities in the series extend into the interior of the TAC, to investigate the extend of this penetration. we made measurements with a long stack of plates. This stack is called TAC #3, although strictly speaking, too long to be considered a TAC. TAC #3 is 4.5 cm long and is instrumented with three single junction pair thermopiles. The junctions of the outer thermopile are located at the edge of the plate. The middle thermopile is 3.5 cm long and centered on the plate. The inner thermopile is 1.5 cm long, also centered on the plate. Measurement of the temperature difference were made with the three thermopile at four drive ratios (0.4, 1.0. 1.7 and 2.3%) and two frequencies (700 and 1100Hz). The results are shown in Figs 19 through 30. The main conclusions to be drawn are : 1) that the irregularities in the data series extend to the locations of all three thermopiles; and 2) the data series are essentially identical in appearance to those obtained from short stacks,

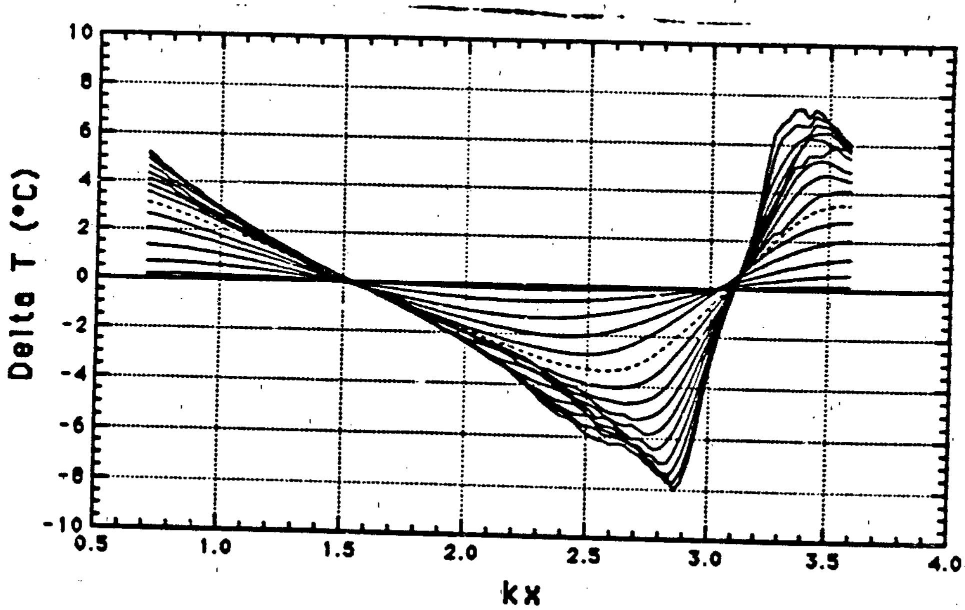

Figure 13 - The temperature difference measured with the outer thermopile on TAC#1

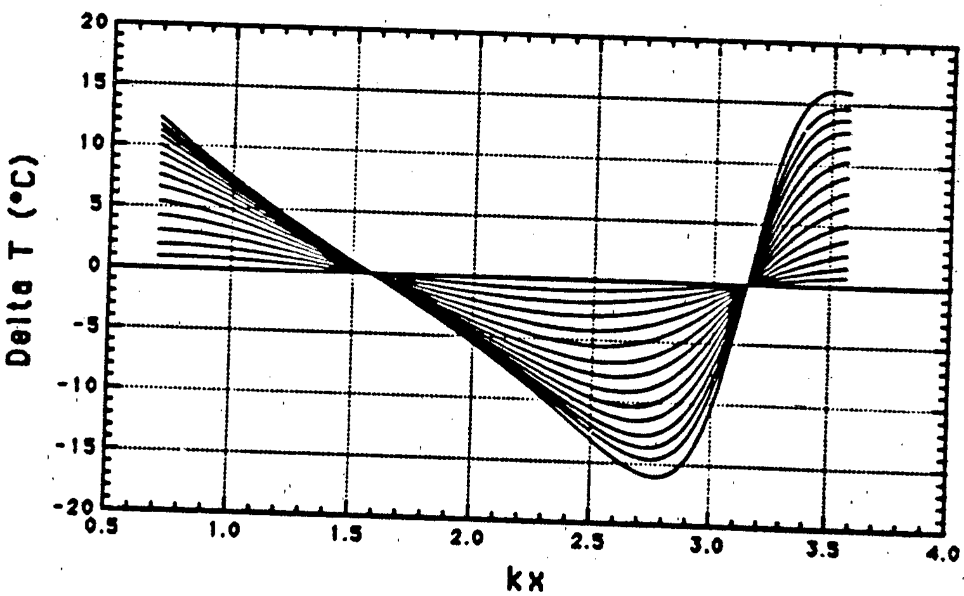

Figure 14 - The theoretical temperature difference at the location of the outer thermopile on TAC#1

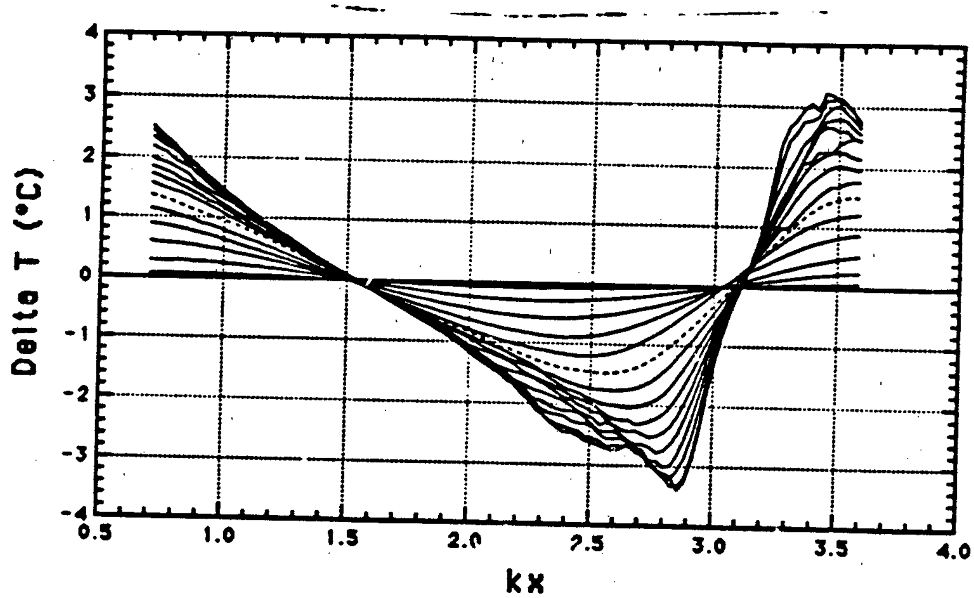

Figure 15 - The temperature difference measured with the inner thermopile on TAC#1

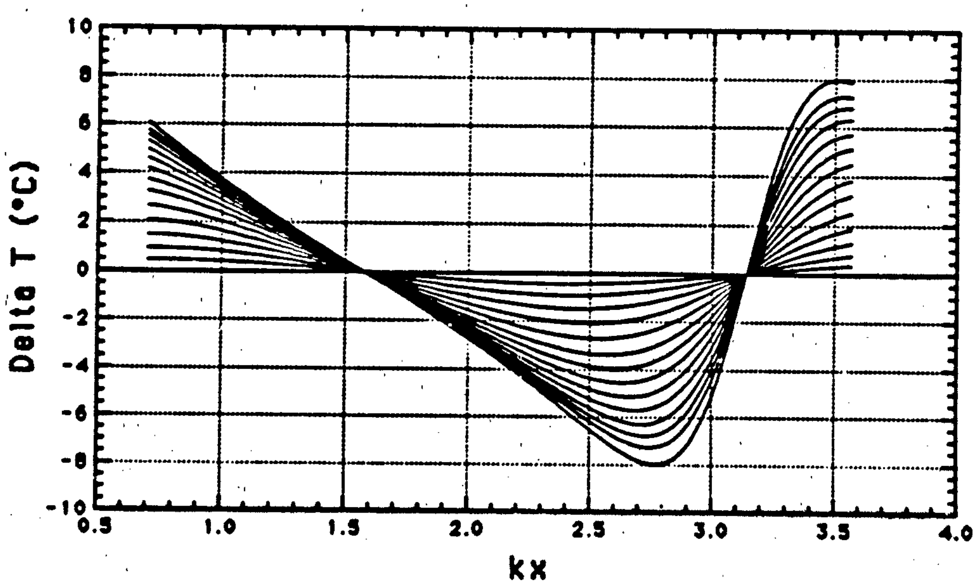

Figure 16 - The theoretical temperature difference at the location of the inner thermopile on TAC#1

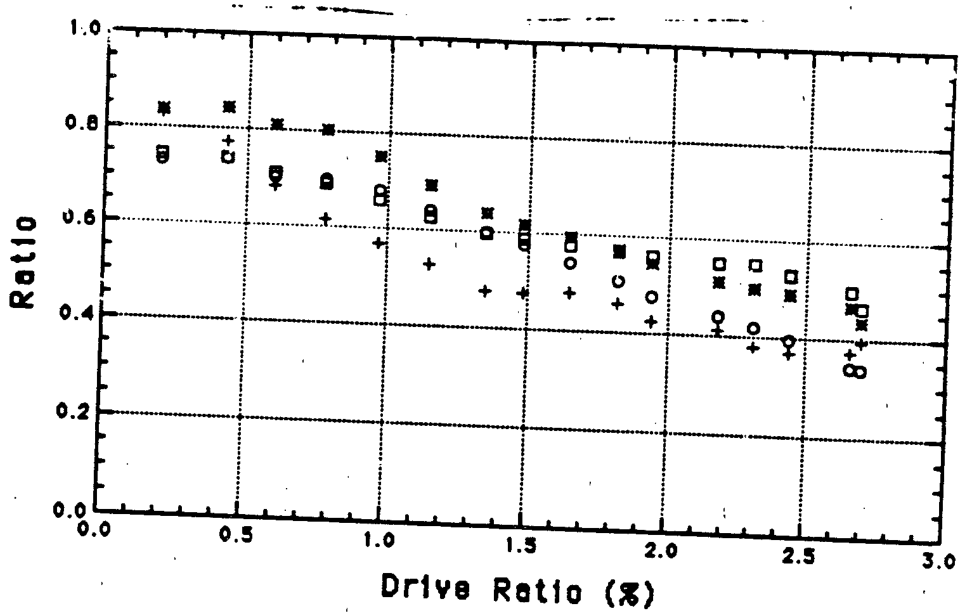

Figure 17 - The dependence of the four ratios on drive ratio (in %) for TAC#1 outer thermopile

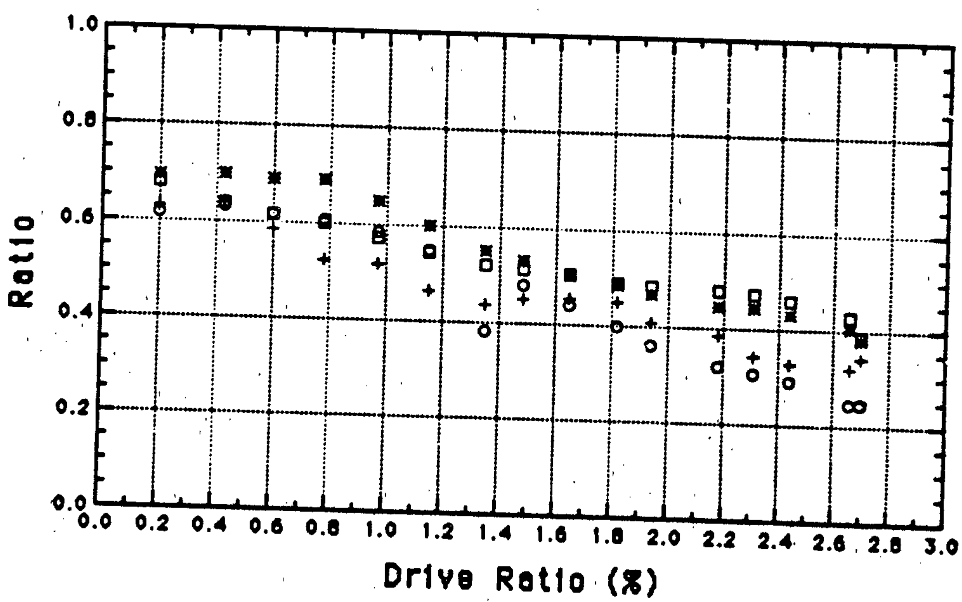

Figure 18 - The dependence of the four ratios on drive ratio (in %) for TAC#1 inner thermopile

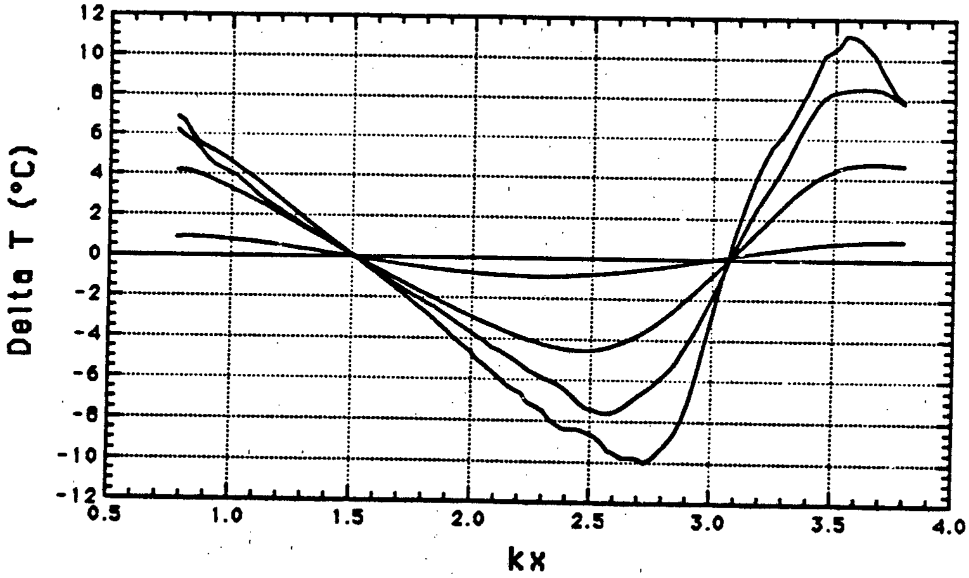

Figure 19 - The temperature difference meas ıred with the outer thermopile on TAC#3 at frequency 700 HZ

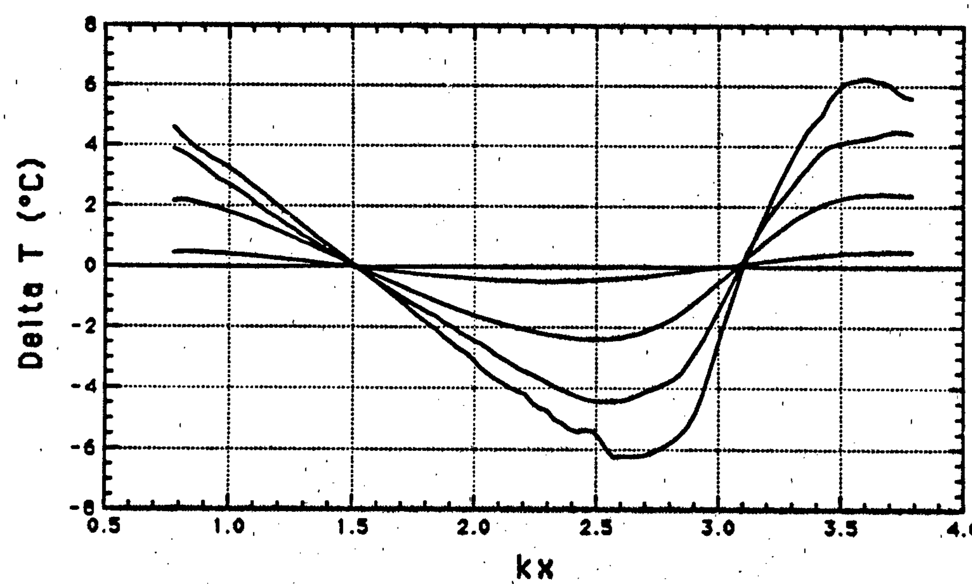

Figure 20 - The temperature difference measured with the middle thermopile on TAC#3 at frequency 700 HZ

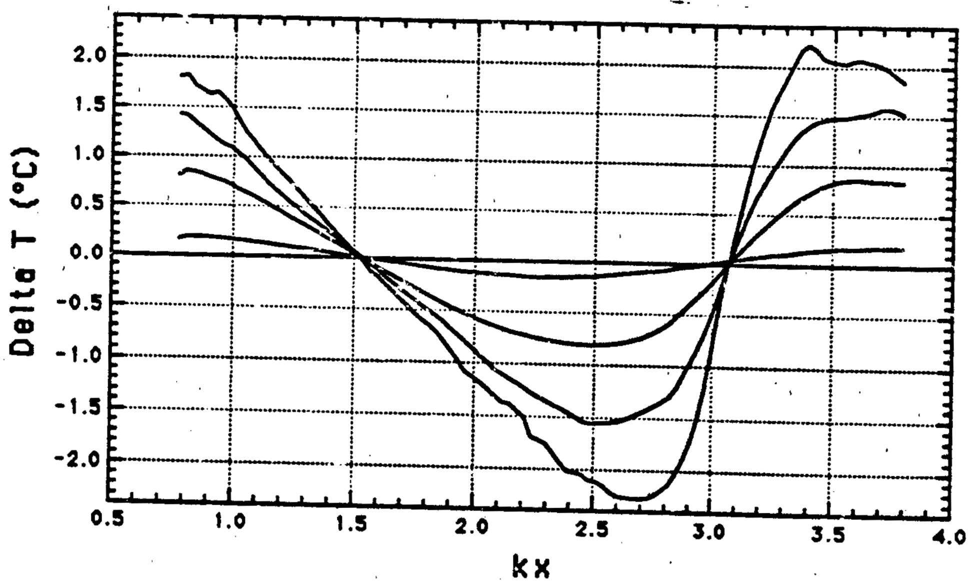

Figure 21 - The temperature difference measured with the inner thermopile on TAC#3 at frequency 700 HZ

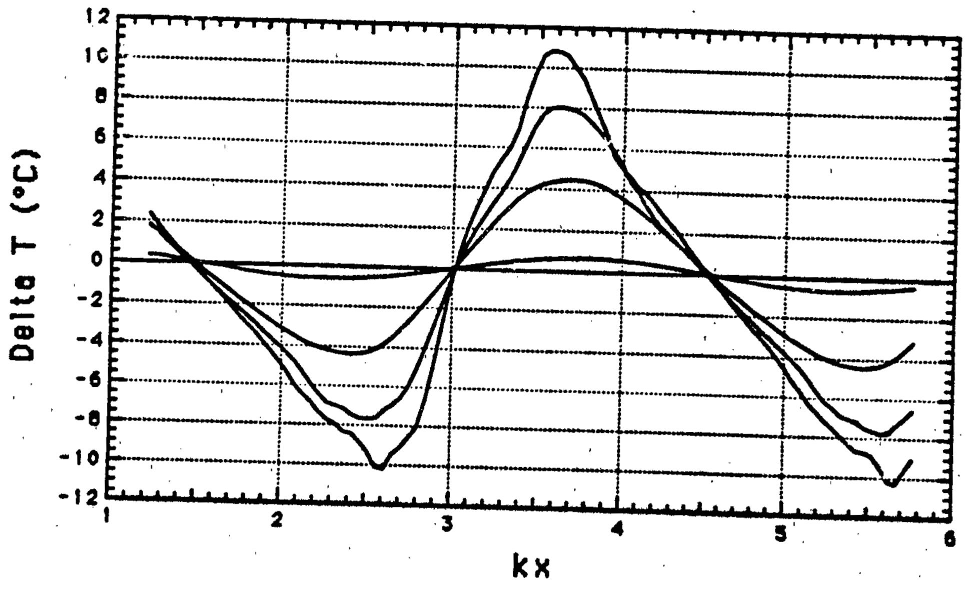

Figure 22 - The temperature difference measured with the outer thermopile on TAC#3 at frequency 1100 HZ

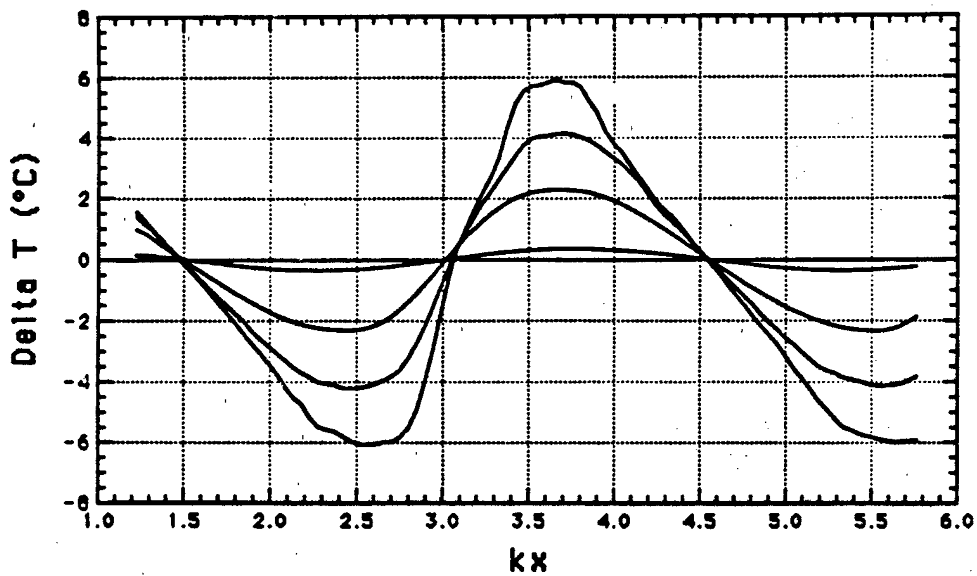

Figure 23 - The temperature difference measured with the middle thermopile on TAC#3 at frequency 1100 HZ

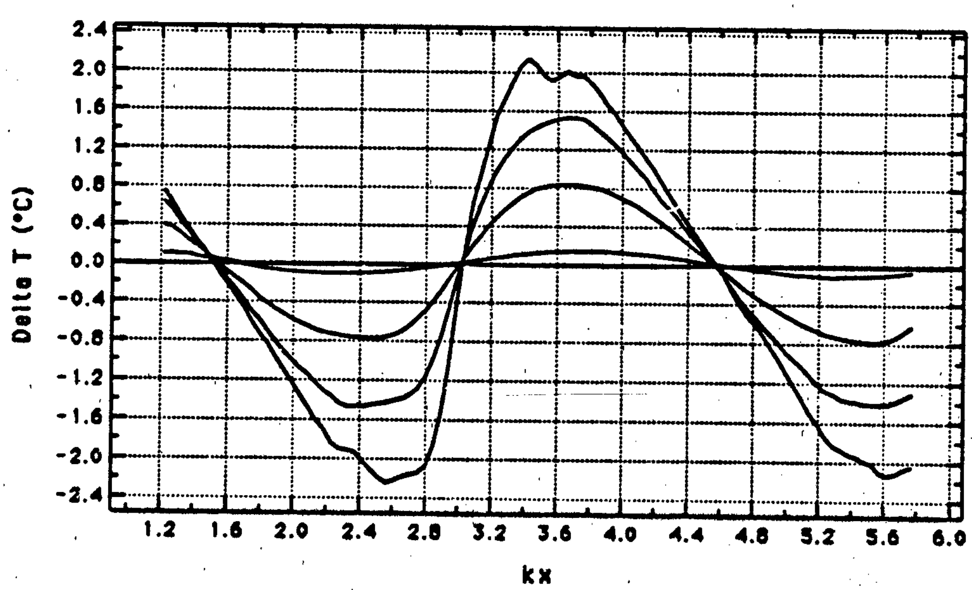

Figure 24 - The temperature difference measured with the inner thermopile on TAC#3 at frequency 1100 HZ

IV. SUMMARY AND CONCLUSION

The purpose of this thesis was to investigate whether or not discrepancies and irregularities observed in previous thermoacoustic couple measurements were artifact of placing the thermopile junctions along the edges of the TAC plates. Measurements were with two stacks, one short and one long, in 2 bar gas for drive ratios ranging up to approximately 2.7%.

The main conclusion is that the behavior observed previously is not isolated to the edge of the plates. It extends at least 1.5 cm into the interior of the plate. The cause of the behavior remains unknown.

LIST OF REFERENCES

1. J. Weatley, T. Hoffler, G. W. Swift, and A. Migliori, *Experiments with an intrinsically irreversible acoustic heat engine..* Journal of the Acoustical Society of America, Vol. 74 (1) , July 1983.

2. Anthony A. Atchley, Thomas J, Hofler, Michael L. Muzzerall, M. David Kite and Ao, *Acoustically generated temperature gradients in short plates* , Journal of the Acoustical Society of America, Vol. 88 (1) , July 1990.

3. L. E. Kinsler, A. R. Frey, A. B. Coppens, and J. V. Sanders, *Fundamental of Acoustics,* Third Edition, John Wiley & Sons, Inc, pp. 210-222, 1982.

4. McCarty R. D. *Thermodynamical Properties of Helium-4 from 2-1500K with Pressure to 1000 Atmospheres,* Washington D.C., NBS Technical Note 631, National Bureau of Standards, 1972.

5. Allegheny Ludlum Steel Corporation, *Stainless Steel Handbook,* Allegheny Ludlum Steel Corporation, 1956.

6. Weast, Robert C., ed., *CRC Handbook of Chemistry and Physics.*

61st ed., Boca Raton, Florida: CRC Press Inc., 1980.

7. El-Hankeem, A. S., *Velocity of Sound in Nitrogen and Argon at High Pressures,* Journal of Chemical Physics, Vol. 42, No. 9, May 1965.

8. Michael Louis Muzzerall, *Investigation of ThermoAcoustic Heat Transport using a Thermoacoustic Couple,* Thesis, Navel Postgraduate School, September 1987.

9. Ao, Chia-Ning., *The Measurements of Thermoacoustic Phenomena Using Thermoacoustic Couples,* Thesis, Navel Postgraduate School, June 1989.

INITIAL DISTRIBUTION LIST

		No. Copies
1.	Defense Technical Information Center Cameron Station Alexandria, Virginia 22304-6145	2
2.	Library, Code 52 Naval Postgraduate School Monterey, California 93943-5100	2
3.	Prof. A. Atcnley, Code PH/Ay Department of Physics Naval Postgraduate School Monterey, CA 93943	3
4.	Dr. T. J. Hofler, Code PH/Hf Department of Physics Naval Postgraduate School Monterey, CA 93943	1
5.	Dr. G. W. Swift Condensed Matter & Thermal Physics Los Alamos National Lab Los Alamos, NM, 87545	1
6.	Dr. Logan E. Hargrove Office of Naval Research Physics Division - Code 1112 800 N. Quincy Street Arlington, VA 22217-5000	1
7.	Prof. S. Garrett, Code PH/Gx Department of Physics Naval Postgraduate School Monterey, CA 93943	1

8. Prof. K. Woehler, Code PH 1
Department of Physics
Naval Postgraduate School
Monterey, CA 93943

9. Liu, Wei-Hsin 1
No. 24, 1038 Lane, Ho-Chang Road
Nan-Tsy Section, Kaohsiung
Taiwan, R. O. C.

10. Library of Chinese Naval Academy 1
P.O. Box 8494 Tso-Ying,
Kaohsiung, Taiwan
Republic of China

11. Library of Chung-Cheng Institute of Technology 1
Tashih, Tao-Yuan, Taiwan
Republic of China

END
FILMED

DATE: 3-92

DTIC